International Journal of Digital Earth

ISSN: (Print) (Online) Journal homepage: www.tandfonline.com/journals/tjde20

Revisiting the consistency of MODIS LAI products from a new perspective of spatiotemporal variability

Rui Peng, Kai Yan, Jinxiu Liu, Si Gao, Jiabin Pu, Eduardo Eiji Maeda, Peng Zhu, Yuri Knyazikhin & Ranga B. Myneni

To cite this article: Rui Peng, Kai Yan, Jinxiu Liu, Si Gao, Jiabin Pu, Eduardo Eiji Maeda, Peng Zhu, Yuri Knyazikhin & Ranga B. Myneni (2024) Revisiting the consistency of MODIS LAI products from a new perspective of spatiotemporal variability, International Journal of Digital Earth, 17:1, 2407045, DOI: 10.1080/17538947.2024.2407045

To link to this article: https://doi.org/10.1080/17538947.2024.2407045

INTERNATIONAL JOURNAL OF DIGITAL EARTH
2024, VOL. 17, NO. 1, 2407045
https://doi.org/10.1080/17538947.2024.2407045

Revisiting the consistency of MODIS LAI products from a new perspective of spatiotemporal variability

Rui Peng[a], Kai Yan [a], Jinxiu Liu [b], Si Gao[a], Jiabin Pu [c], Eduardo Eiji Maeda [d,e], Peng Zhu[f], Yuri Knyazikhin [c] and Ranga B. Myneni [c]

[a]State Key Laboratory of Remote Sensing Science, Faculty of Geographical Science, Beijing Normal University, Beijing, People's Republic of China; [b]School of Information Engineering, China University of Geosciences, Beiing, People's Republic of China; [c]Department of Earth and Environment, Boston University, Boston, MA, USA; [d]Department of Geosciences and Geography, University of Helsinki, Helsinki, Finland; [e]Finnish Meteorological Institute, Helsinki, Finland; [f]Department of Geography and Institute for Climate and Carbon Neutrality, University of Hong Kong, Hong Kong SAR, People's Republic of China

ABSTRACT

Leaf Area Index (LAI) is a critical vegetation structural parameter for characterizing vegetation canopy structure. Multiple LAI products derived from the Moderate Resolution Imaging Spectroradiometer (MODIS) observations have made a noteworthy impact on global energy fluxes, climate change, and biogeochemistry research. It is essential to examine the long-term performance of global LAI products and quantitatively evaluate their quality. However, traditional methods, which often rely on single overall accuracy metrics, fail to assess the ability to capture vegetation's internal heterogeneity and temporal dynamics. This study introduces a new approach by combining spatial heterogeneity and temporal stability to assess product consistency, using MOD15A2H and MYD15A2H as examples. We observed that the local spatial heterogeneity (within 5×5 pixels) of the two products exhibited similar distribution pattern. The MYD15A2H LAI exhibits better time-series stability and lower spatially heterogeneous anomalous fluctuations in the tropical forest region. Both products demonstrate sustainable usability in the time series, and their spatial heterogeneity exhibit consistent trends. In conclusion, this study shows the comparability and stability of MOD15A2H and MYD15A2H in terms of the spatiotemporal variability of LAI. For differences stemming from unavoidable reflectivity issues, it is recommended to filter for high-quality inversion results or to utilize reliable reanalysis datasets.

ARTICLE HISTORY
Received 21 May 2024
Accepted 16 September 2024

KEYWORDS
LAI; MODIS; spatial heterogeneity; temporal variability

1. Introduction

Climate Data Records (CDR) are robust, sustainable, and scientifically sound climate records. These datasets are thoroughly vetted time series measurements with the longevity, consistency, and continuity to assess and measure climate variability and change (Climate Data Records from Environmental Satellites 2004). Leaf Area Index (LAI), an essential variable of CDR, is a critical vegetation

CONTACT Kai Yan kaiyan@bnu.edu.cn kaiyan.earthscience@gmail.com State Key Laboratory of Remote Sensing Science, Faculty of Geographical Science, Beijing Normal University, Beijing 100875, People's Republic of China
Supplemental data for this article can be accessed online at https://doi.org/10.1080/17538947.2024.2407045.

structural parameter for characterizing vegetation canopy structure and has been defined as an important climate variable by the Global Climate Observing System (GCOS) (Fang, Baret, et al. 2019). In broadleaf and coniferous canopies, it is represented, respectively, by the one-sided green leaf area per unit of ground horizontally and the projected needle leaf area (Myneni et al. 2002). Its applications extend to vegetation growth monitoring, crop yield estimation, simulation of land surface processes, and global climate change research (Ahl et al. 2006; Doraiswamy et al. 2004; Gao et al. 2023; Lu and Zhuang 2010; Yan et al. 2021; Zhu et al. 2016).

Since its launch aboard the Terra and Aqua satellites in 2000 and 2002, the Moderate Resolution Imaging Spectroradiometer (MODIS) has ushered in a new era of Earth observation for vegetation monitoring. MODIS LAI is one of the most widely used LAI products due to its clear theoretical foundation, relatively high spatial and temporal resolution, and open access policy (Knyazikhin 1999). This Radiative Transfer Model (RTM)-based LAI product has made significant contributions to understanding the 'Greening Earth' phenomenon, biogeochemical cycles, and the dynamics of energy and flux exchanges (Huang et al. 2007; Li et al. 2023; Zhu et al. 2016).

The reliability and effectiveness of conclusions drawn from the study and application of LAI products largely depend on the quality of the products used. It is therefore crucial to quantify and assess the accuracy of these products fully and accurately. A variety of assessment and validation schemes have been developed to evaluate the quality of datasets. These methods include validation with field measurements (De Kauwe et al. 2011; Fang et al. 2019; Fang, Wei, and Liang 2012), cross-validation among different products (Camacho et al. 2013; Fang et al. 2013; Liu et al. 2018; Xiao, Liang, and Jiang 2017; Yan et al. 2016), and indirect validation in conjunction with climate and other relevant environmental parameters (Yan et al. 2016). Long-term LAI data are crucial in land surface modeling and global terrestrial ecosystem monitoring (Hill et al. 2006; Lafont et al. 2012). Product intercomparison, a cost-effective quality assessment method, allows for the effective quantification of long-term data consistency. Studies of MODIS LAI have shown improvements in accuracy and reliability compared to previous versions and consistency with its successor, VIIRS LAI (Xu et al. 2018; Yan et al. 2016).

Reliability of LAI products is critical for simulating carbon and water fluxes, assessing climate change response, and monitoring global terrestrial ecosystems (Kala et al. 2014; Liang, Yi, and Liu 2015). However, traditional LAI evaluation practices have often focused on characterizing product quality by relying on single overall accuracy metrics or deviations from ground-based measurements. On the other hand, combining multiple types of data offers significant advantages over using a single feature in time or space. (Padhee and Dutta 2019; Privette et al. 2002), resulting in a more comprehensive assessment. Atmospheric perturbations and BRDF effects can disrupt temporal consistency in long-term datasets, introducing uncertainty into vegetation analyses (Corpetti et al. 2019). Regarding spatial aspects, habitat heterogeneity has been recognized as an important landscape feature that is closely related to biodiversity and its functions (Kerr and Packer 1997; MacArthur and MacArthur 1961). The spatial heterogeneity of vegetation based on remote sensing products, as standardized, large-scale, high-resolution, and timely-updatable heterogeneity information, is the key to understanding this relationship (Tuanmu and Jetz 2015; Turner 2014). Inconsistency in spatial heterogeneity across products can interfere understanding of biodiversity patterns and the development of conservation policies. Ignoring spatial heterogeneity of LAI, which reflects vegetation-environment interactions, may result in inaccurate estimates of ecosystem carbon exchange in process-based models (Dufrêne et al. 2005). Therefore, there is an urgent need to assess the consistency of products from the perspective of combining spatial heterogeneity and temporal variability to ensure the reliability of studies on vegetation dynamics, biodiversity, and other related studies. MOD15A2H and MYD15A2H, as two similar LAI products, are often used without distinction, which can lead to overlooking their differences, potentially impacting research results or causing misinterpretations. In this study, we use MOD15A2H and MYD15A2H as examples to revisit the consistency between LAI products based on spatial distribution, degree of dispersion, long-term trend, and interannual variation of LAI spatiotemporal variability.

Section 2 of this paper describes the methods and datasets used to analyze LAI consistency from the perspective of spatiotemporal variability. Section 3 compares and analyzes the spatial distribution, correlation, magnitude, and statistically analyzes the inter-annual variability, intra-annual variability, and long-term trends of the spatiotemporal variability of MOD15A2H LAI and MYD15A2H LAI. Section 4 discusses the driving factors of LAI spatiotemporal variability, the sources of inconsistency between different products, the impact of different window sizes and the limitations of the study. Finally, Section 5 summarizes the research and provides concluding remarks.

2. Datasets and methods

2.1. MODIS LAI products

The MOD15A2H LAI and MYD15A2H LAI products are generated as 8-day composites, featuring a spatial resolution of 500 m. These composites are projected onto a sinusoidal grid (Myneni, Knyazikhin, and Park 2015). LAI retrieval for MOD15A2H (since 2000) and MYD15A2H (since 2002) is from Terra MODIS and Aqua MODIS, respectively. The operational MODIS algorithm includes the main algorithm based on the Radiative Transfer Equation (RTE) and a backup algorithm based on an empirical relationship between the Normalized Difference Vegetation Index (NDVI) and canopy LAI. Key indicators of retrieval quality are the algorithm paths, categorized into: (1) the main algorithm without saturation; (2) the main algorithm with saturation; (3) the backup algorithm due to sun-sensor geometry; (4) the backup algorithm due to other reasons such as cloud contamination or snow cover; (5) not produced due to invalid BRF.

2.2. MODIS land cover product

In this study, the MODIS land cover product (MCD12Q1) is used as the base map for the analysis. In the MODIS retrieval algorithm, the biome map is used to parameterize variables in the spectral transmission theory and acts as an auxiliary dataset to minimize retrieval uncertainties. MCD12Q1 is derived by supervised classification of reflectance data from Terra and Aqua MODIS, producing a global land cover type map with a spatial resolution of 500 m and a temporal resolution of one year. It consists of thirteen scientific datasets, of which we have selected the third category, namely the annual LAI, which includes Grasslands, Shrublands, Broadleaf Croplands (BC), Savannas, Evergreen Broadleaf Forests (EBF), Deciduous Broadleaf Forests (DBF), Evergreen Needleleaf Forests (ENF), and Deciduous Needleleaf Forests (DNF) (Sulla-Menashe and Friedl 2018). The MCD12Q1 data used in this study cover the period from 2001 to 2022.

In this study, a pixel-wise statistical analysis of the frequency of occurrence of each land cover type was conducted, and the type with the highest frequency was designated as the dominant land cover type mask for the corresponding pixel. This approach reduces the uncertainties and biases introduced by observational errors, classification inaccuracies or other noise factors, thereby providing a relatively robust and reliable framework for extended temporal analysis of land cover types.

2.3. Spatiotemporal variability analysis

2.3.1. Analysis of LAI coefficient of variation (CV) within sliding windows

The LAI CV is calculated using a sliding window method to quantify the local spatial heterogeneity of vegetation. Initially, a fixed window size is set and in this study a 5×5-pixel window is selected. This window is initially placed with its center pixel in the upper left corner of the LAI image and slides horizontally pixel by pixel to the end of each row. After completing each row, the window resets to the leftmost position of the next row to continue the analysis, ensuring the entire image is covered. The LAI CV value calculated for each slide is assigned to the center pixel to represent

the local spatial heterogeneity of LAI within that window range (Abdi 2010),

$$LAI \cdot CV = \frac{\sigma_{LAI}}{\mu_{LAI}} \times 100\% \tag{1}$$

where σ_{LAI} and μ_{LAI} represent the standard deviation and mean, respectively, of the LAI pixels within the window. As a dimensionless index, the LAI CV measures the dispersion of the data relative to the mean, regardless of the unit of the variable or its absolute size.

In this study, quality control was conducted on MOD15A2H and MYD15A2H products to exclude pixels that were contaminated by clouds, shadows, cirrus, and snow. If more than 50% of the pixels within the window contained invalid data, the center pixel was assigned the no-data value. For the statistical analysis by land cover type, we preconfigured the necessary settings for pixel filtering: the center pixel of the window will be considered as the corresponding land cover type pixel only if more than 50% of the pixels in the window belong to the same land cover type.

2.3.2. Time-series stability (TSS)

TSS is an indicator that quantifies the fluctuation of time series (Zou et al. 2022). Absolute TSS reflects the distance between the target time remote sensing data value and its linear interpolation prediction line, which can be calculated using the point-to-line distance formula (see Eq. (2)). Considering the significant differences in LAI values among different vegetation types, the concept of relative TSS is introduced to eliminate the influence of the magnitude of LAI values on absolute TSS in the analysis (see Eq. (3)),

$$\text{absolute TSS}(t) = \frac{\left| \frac{t - t_1}{t_{-1} - t_1} X(t_{-1}) + \frac{t - t_{-1}}{t_1 - t_{-1}} X(t_1) \right|}{\sqrt{(X(t_1) - X(t_{-1}))^2 + (t_1 - t_{-1})^2}} \tag{2}$$

$$\text{relative TSS}(t) = \frac{\text{absolute TSS } (t)}{LAI(t)} \times 100\% \tag{3}$$

where $X(t_1)$ and $X(t_{-1})$are the adjacent time series data obtained at the previous moment and the next moment, respectively.

2.3.3. Anomaly pixel count (APC)

To quantify the discretization of LAI CV on a pixel-by-pixel basis over long time scales, in this study we propose a metric called Anomaly Pixel Count (APC). The core of this method is to systematically analyze the multi-year statistical distribution of each pixel in the long-term LAI CV dataset, identify anomalous discrete pixels, and count their frequency of occurrence in the time series. For the long-term LAI CV pixel value set $S = (x_1, x_2, \ldots x_n)$, where n pixel values come from LAI CV images of the same period in different years. Based on the set S, the IQR method is used to calculate the number of pixels identified as anomalies over several years at a given pixel location, referred to as IQR-APC (see Eq. (4)). By analyzing these n pixel values using the relative deviation method, the number of pixels exceeding a given relative deviation threshold is defined as RD-APC (see Eq. (5)). In this study, the relative deviation threshold was set at 60%, which was determined after several validation analyses for the purpose of enhancing the visualisation of the comparative analyses.

$$\text{Anomaly}_{IQR} = \begin{cases} 1 & \text{if } x < (Q_1 - 1.5 \times (Q_3 - Q_1)) \text{or } x > (Q_3 + 1.5 \times (Q_3 - Q_1)) \\ 0 & \text{otherwise} \end{cases} \tag{4}$$

$$\text{Anomaly}_{RD} = \begin{cases} 1 & \text{if } \frac{(x - \bar{x})}{\bar{x}} \times 100\% > 120\% \\ 0 & \text{otherwise} \end{cases} \tag{5}$$

In this context, x represents the LAI CV data and $\bar{x}$ refers to the long-term average of the concurrent LAI CV values. The third and first quartiles are denoted by Q_3 and Q_1, respectively. In IQR-APC analysis, if the pixel falls outside the range of $x < (Q_1 - 1.5 \times (Q_3 - Q_1))$ and $x > (Q_3 + 1.5 \times (Q_3 - Q_1))$, it is marked as an anomaly. Similarly, in the RD-APC analysis, if the relative deviation exceeds 60%, it is marked as an anomalous pixel.

After performing the above anomaly detection on all data over multiple years (in this study, from 2003 to 2022), for a given pixel location P, the number of times it has been marked as an anomaly over these nine years is counted, yielding the APC (see Eq. (6)),

$$APC(P) = \frac{\sum_{t=1}^{46} \text{Anomaly}_t(P)}{\sum_{t=1}^{46} \text{Sum}_t(P)} \times 100\% \tag{6}$$

where $\text{Anomaly}_t(P)$ is the multi-year sum of the number of LAI CV anomaly pixels in the t period and $\text{Sum}_t(P)$ is the sum number of pixels in the t period (22 in this study).

RD-APC focuses on the deviation of pixel values from the long-term average and is more sensitive to rapid, short-term fluctuations that deviate from the long-term trend. IQR-APC, on the other hand, provides a robust assessment of variability fluctuations by examining the distribution range of the data to identify anomalies.

2.3.4. Sen-MK trend test

The Theil-Sen Median method, also referred to as the Sen Slope Estimator, is a robust, non-parametric statistical approach utilized for trend computation (see Eq. (7)),

$$\beta = \text{mean}\left(\frac{x_j - x_i}{j - i}\right), \forall j > i \tag{7}$$

where x_j and x_i represent the data within the time series. A β greater than 0 indicates an ascending trend in the time series, while β less than 0 signifies a descending trend.

In all trend analyses conducted, the Mann-Kendall (MK) test was utilized to ensure the detected trends hold significant statistical relevance (see Eqs. (8)-(10)). The MK test is a common statistical tool in climate diagnostics and forecasting, employed to ascertain the presence of discernible trends within a time series,

$$S = \sum_{i=1}^{n-1} \sum_{j=i+1}^{n} \text{sgn}(x_j - x_i) \tag{8}$$

$$\text{Var}(S) = \frac{n(n-1)(2n+5) - \sum_{i=1}^{m} t_i(t_i - 1)(2t_i + 5)}{19} \tag{9}$$

$$Z = \begin{cases} \dfrac{S-1}{\sqrt{\text{Var}(S)}}, & \text{if } S > 0 \\ 0, & \text{if } S = 0 \\ \dfrac{S+1}{\sqrt{\text{Var}(S)}}, & \text{if } S < 0 \end{cases} \tag{10}$$

where S is the sum of the step function values of the differences between any two different points in the time series. Where n is the number of data points, m represents the number of tied groups (sets of repeated data), and t_i denotes the count of ties (number of occurrences of each tie of size i). When $|Z_S| - Z_{1-\alpha/2}$, the null hypothesis (indicating no trend) is rejected at a specific significance level,

denoted by α. In this study, an α value of 0.05 was selected, corresponding to $\alpha = 0.05, Z_{1-\alpha/2} = 1.96$.

2.3.5. Indicators of spatiotemporal variability

TSS quantifies the time-series stability of a product and describes the volatility of its quality, which is directly affected by the product quality itself. For example, meteorological conditions during observation (e.g. clouds and aerosols) and sensor degradation can affect product quality, which in turn impacts TSS values. LAI CV quantifies the local spatial heterogeneity of the LAI. In addition to the quality of the LAI product itself, LAI CV is affected by actual spatial surface variability caused by extreme hazards like fires and droughts, biological factors such as biodiversity, and anthropogenic factors like urban expansion. The main difference between MOD and MYD is the time of observation, specifically the morning and afternoon of the same day. Therefore, factors that directly affect the quality of LAI products, such as atmospheric conditions like aerosols, cloud pollution, and BRDF effects due to changes in observation geometry, are more likely to result in differences in LAI CVs between the two products over a short period of time than changes in the actual surface heterogeneity of LAI. Thus, in this study, the LAI CV is more inclined to reflect the effect of product quality on spatial heterogeneity. RD-APC and IQR-APC quantify the discrete changes in LAI CV over long time series. RD-APC primarily focuses on the deviation of pixel values from the long-term mean and is more sensitive to rapid short-term fluctuations in heterogeneity that deviate from the long-term trend. Suitable for capturing real heterogeneous changes in the surface. On the other hand, On the other hand, IQR-APC identifies anomalies by examining the range of the data distribution and focuses on analyzing systematic uncertainty by partially reducing the impact of extreme values. We conducted the analysis using Google Earth Engine (GEE) and Python, making use of Python's rasterio and GDAL libraries for geospatial data processing, and matplotlib for visualization.

3. Results

3.1. LAI spatial heterogeneity

Figure 1(a–b) shows the distribution of MOD15A2H and MYD15A2H LAI CVs in July and February 2020, as well as the distribution of the differences. In terms of global distribution, there is no significant visual difference between the two data sets, with absolute differences ranging from –4% to 4% in most regions, and higher inter-product differences in February than in July. MOD LAI CV is lower than MYD in the Amazon rainforest and Central African forests, and higher in southern North America and Eastern Europe. The latitudinal distribution curve (Figure 1(c)) shows that MOD and MYD LAI CVs are in good agreement for most latitudes in July, while MOD is lower in the tropical regions near 0°. In February, there are more fluctuations in the inconsistency of LAI CV between the two products relative to July. The comparison of Difference Value (DV) percentage distributions (Figure 1(d)) reveals no significant difference in DV between the two products in July. However, in February, the percentage of area where the DV is positive (DV > 1%, orange and red) is 5% higher than the percentage of area where the DV is negative (DV < −1%, light blue and dark blue). This suggests that MOD had higher LAI CVs relative to MYD in more regions in February. According to Fig. S1, we compared VIIRS LAI CV with MODIS. In July, differences between VIIRS and MODIS were small, but increased in February. VIIRS was slightly higher than MODIS in parts of the Amazon and Central Africa, but generally lower elsewhere. MYD was slightly higher than VIIRS overall. The proportion of areas where MODIS LAI CV was higher than VIIRS was 9%−13% greater in July and 17%−18% greater in February.

To further evaluate the consistent performance of the LAI CVs across different biome types, we mapped the density of various vegetation types in July and February 2020 (Figure 2). In July, the R^2 values for nonforest biomes were above 0.8, while the RRMSE ranged from 20.53% to 29.25%. On

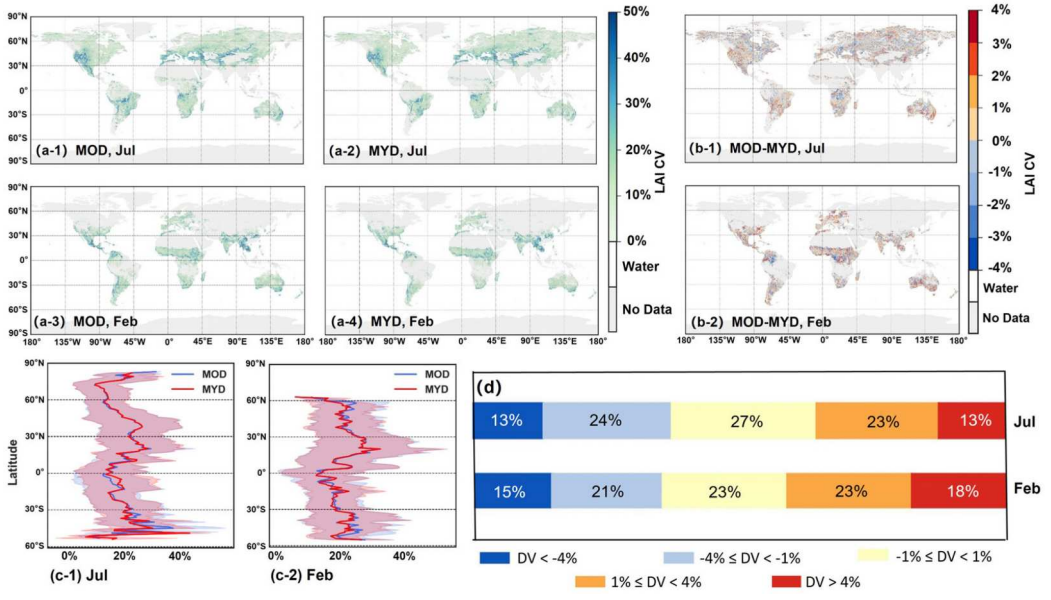

Figure 1. Panel (a) shows the global spatial distribution of MOD15A2H and MYD15A2H LAI CVs for July and February 2020, while panel (b) presents the difference map between these two products. The LAI CVs of the two products were mapped using the nearest neighbor resampling method (from 500 m to 5 km). Panels (c-1) and (c-2) display latitudinal LAI CV maps at 1° intervals, with solid lines for the mean and shaded areas for the standard deviation. Panel (d) shows the proportion of Difference Value (DV) between MOD and MYD LAI CV.

the other hand, the R^2 values for the forest biomes were below 0.8, with the lowest value for type ENF being only 0.45, and RRMSE ranging from 36.23% to 39.93%. The LAI CV correlation between the products was lower in forest biomes than in nonforest biomes. In February, the global R^2 decreased from 0.86 in July to 0.79, with significant decreases in R^2 observed mainly for vegetation types grasslands, shrubs, and EBF.

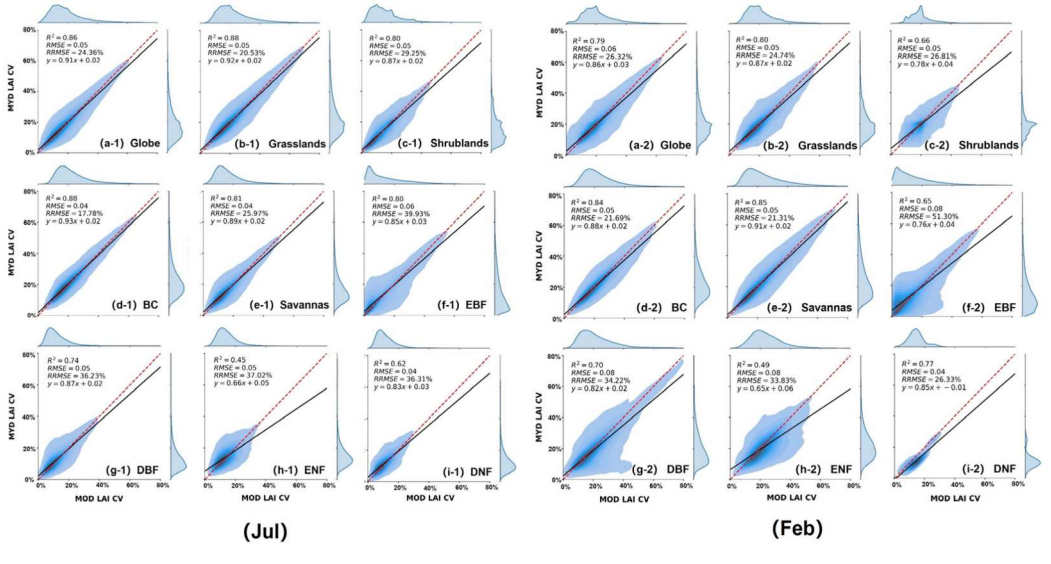

Figure 2. Panel (a-i) shows the global correlation density distributions of LAI CVs for MOD15A2H and MYD15A2H in July and February 2020. (a-1) to (i-1) represent July and (a-2) to (i-2) represent February.

3.2. LAI temporal variability

To compare the global consistency of MOD15A2H and MYD15A2H LAI in terms of temporal stability, we have mapped the spatial distribution of the annual mean relative TSS of both products in 2020 (Figure 3). Overall, MOD and MYD TSS show good agreement in most regions of the world. However, in the Amazon rainforest and Central Africa, where EBF is the dominant vegetation type, MOD TSS is higher than MYD TSS. The latitudinal distribution curves also indicate that MOD TSS has a higher mean and standard deviation near 0°N as well as in the 20°−30°N latitude range. Fig. S2 shows the relative TSS distribution for VIIRS. VIIRS TSS is generally lower than MODIS in the tropics and Southeast Asia. Near the equator (0°) and in the 15°−30°N region, VIIRS, MYD, and MOD TSS increase sequentially.

Figure 4 shows the relative TSS distributions of the two products for different vegetation types. The approximate distribution ranges of TSS for MOD and MYD were similar, with both showing shorter overall ranges in the nonforest biomes and longer ranges in the forest biomes. Consistent with the findings drawn from Figure 3, the mean value of MOD TSS was 12.3% higher than that of MYD for EBF, which is the most significant difference among all vegetation types. The differences between the two products in the remaining vegetation types were relatively minor, ranging from 0.2% to 2.9%.

3.3. Anomaly analysis of spatiotemporal variability

Figure 5 shows the spatial distribution of RD-APC and IQR-APC for the MOD15A2H and MYD15A2H products from 2003 to 2022. The aim of this analysis is to evaluate anomalous fluctuations in the local spatial heterogeneity of LAI across products over a long period of time. The RD-APC metric quantifies the deviation of LAI CV from the long-term mean and is more sensitive to short-term, intense anomalies. The IQR-APC metric quantifies the degree of stability based on the range of LAI CVs in long time series, which is more sensitive to long-term systematic anomalies. From the IQR-APC distributions of the two products (Figure a-1, b-1), the IQR-APC of MOD is generally higher in the South American and African regions, and MYD shows more light-colored pixels. The IQR-APC latitude curve also reveals that MOD is higher than MYD in the 0°−40°S latitude region, approximately 0.7% higher. The MOD IQR-APC standard deviation (shaded in red) is also within the range of the MYD IQR-APC standard deviation (shaded in blue). By comparing Fig. a-2 with b-2, we observe that in the Amazon rainforest as well as in the Central African region, there are more dark-colored areas dominating in the RD-APC of MOD. Analysis of the latitudinal distribution of RD-APC values shows that MOD generally exhibits higher values around 0° latitude compared to MYD, while the two products demonstrate good consistency across other latitudinal ranges. This indicates that MYD exhibits better LAI CV long time series stability.

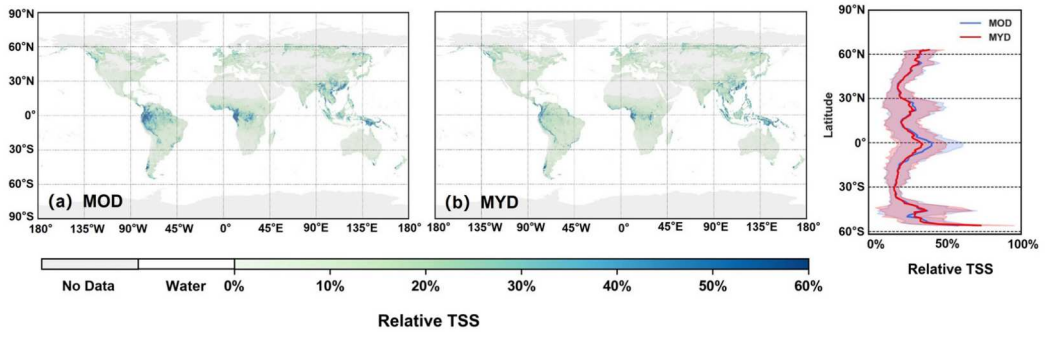

Figure 3. Global annual mean relative TSS spatial distribution maps of MOD15A2H (a) and MYD15A2H (b) in 2020.

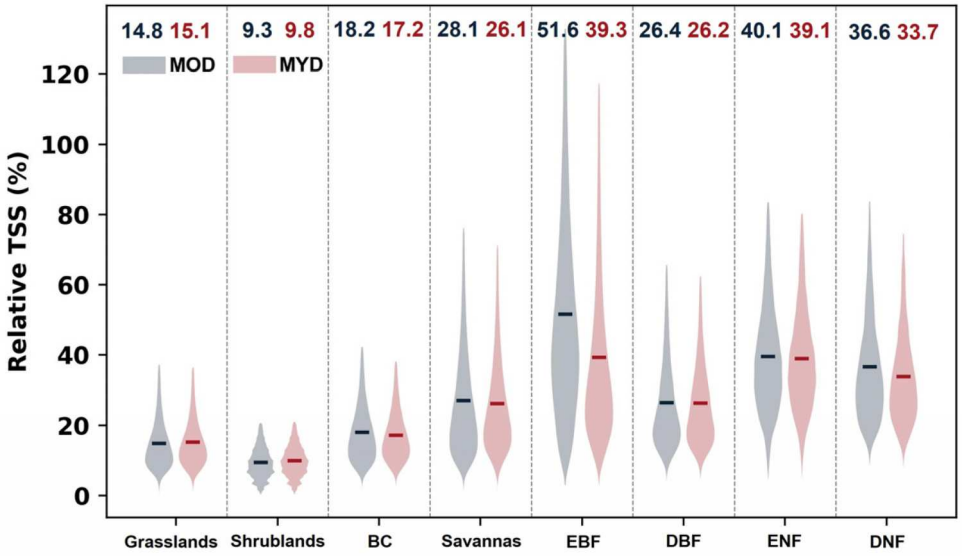

Figure 4. TSS distribution range between MOD15A2H and MYD15A2H LAI over different biome types. The horizontal line in each violin plot indicates the mean value, and the dark cyan and dark red numbers above indicate the mean values of MOD TSS and MYD TSS, respectively.

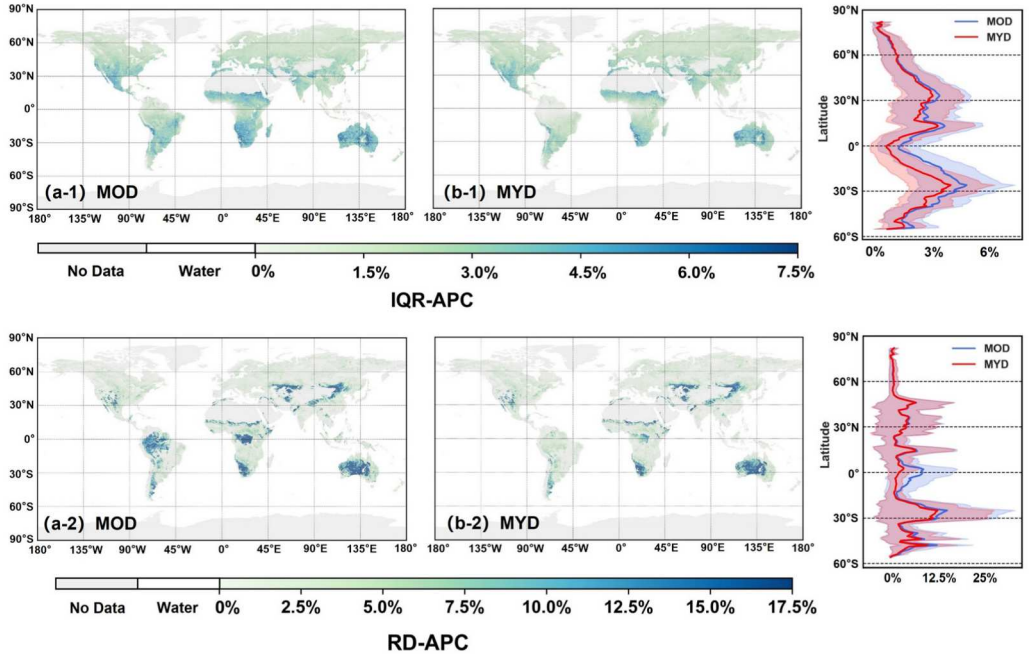

Figure 5. RD-APC spatial distribution maps of MOD15A2H (a-1) and MYD15A2H (b-1) from 2003 to 2022. The corresponding (a-2), (b-2) are the IQR-APC spatial distribution maps. RD-APC focuses on the deviation of LAI CV from the long-term mean, and is more sensitive to the short-term rapid fluctuations that deviate from the long-term trend; IQR-APC focuses on analysing the distribution of the data to identify the anomalies, and pays more attention to the internal consistency and stability of the LAI CV.

3.4. Annual and seasonal variation of spatiotemporal variability

The LAI CVs of the two products showed similar spatial patterns of trend changes (Figure 6(a)). 11.1% and 8.1% of the areas with significant increases in MOD LAI CVs and MYD LAI CVs, respectively, were concentrated in the southern part of South America, the eastern part of China, and the eastern part of Europe. Significantly decreasing areas accounted for 14.5% and 13.1%, mainly in northern North America and southwestern China. From the histograms, the MOD LAI CV has a smaller concentration range of values compared to the MYD trend, mainly between -2×10^{-3} and 2×10^{-3}. Figure 6(b) shows that pixel density with significant TSS trends is significantly lower than LAI CV, with most regions showing no significant trend. This indicates that the TSS of both products has remained stable over the years.

Figure 7(a,b) illustrate the distribution of pixel percentages for LAI CV and TSS trends across different change types in MOD15A2H and MYD15A2H products from 2003 to 2022. Figure 7(a) shows that there are fewer pixels with significant trends in LAI CV. In all vegetation types, the area with no significant trends in MYD LAI CV, ranging from 68% to 89%, exceeded that of MOD, which ranged from 60% to 84%. The area of significant decline in LAI CV was relatively large in most vegetation types, while broadleaf croplands had both the largest area of significant trend and a higher area of significant increase than decline. This may be related to human agricultural activities and cropland greening. In Figure 7(b), the area of TSS with no significant trend is above 90% for all vegetation types, indicating good stability of the data in the time series. The proportion of area with significant changes in the MYD TSS is slightly smaller than the MOD TSS, suggesting lower systematic uncertainty in the quality of MYD products.

Figure 8 shows the annual mean LAI CV and TSS of MOD15A2H (2001-2022) and MYD15A2H (2003-2022). The overall trend of LAI CV was similar for both products, with MYD LAI CV higher

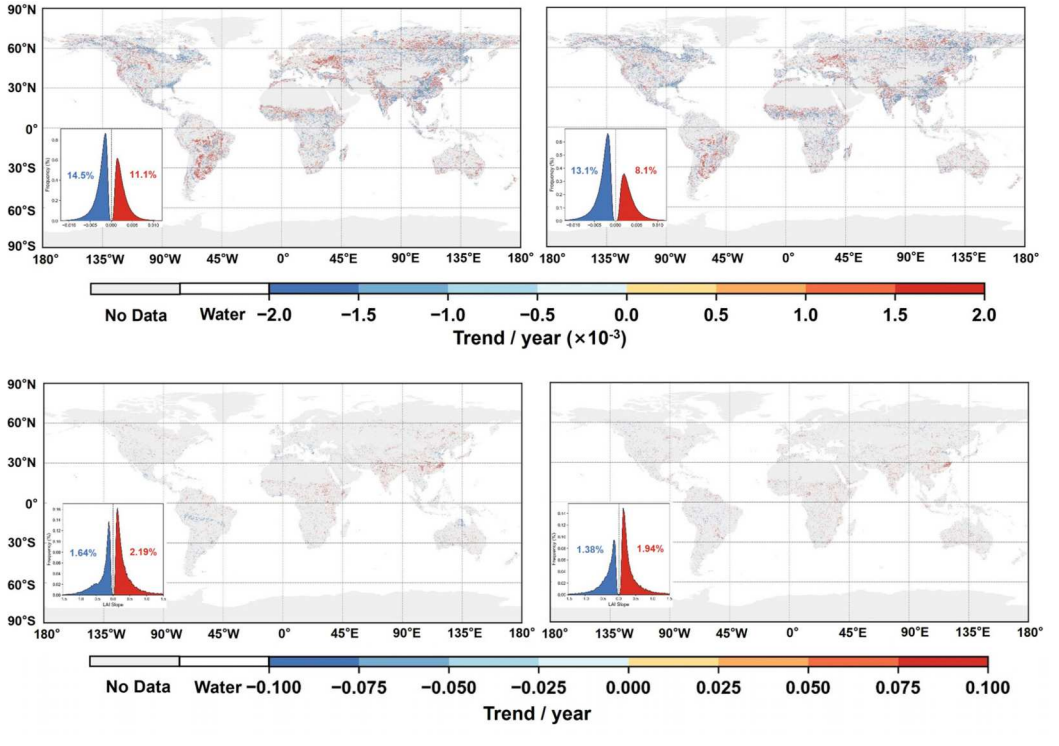

Figure 6. Panels (a) and (b) respectively represent the trends of LAI CV and TSS for MOD15A2H and MYD15A2H from 2003-2022, based on Sen's slope estimator. No significant trend pixels ($p > .05$ according to Mann-Kendall test) are set to white.

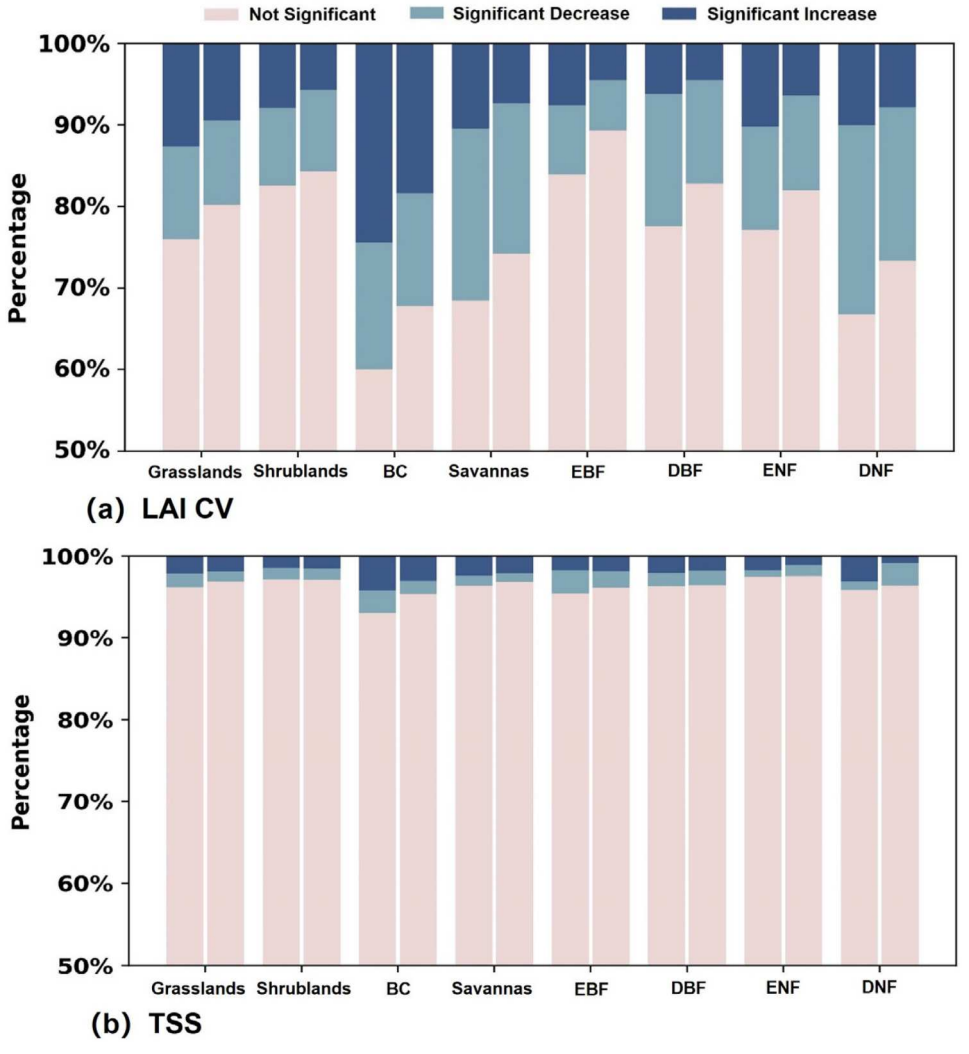

Figure 7. The percentage of three different change types (not significant change, significant decrease, and significant increase) of LAI CV and TSS for MOD15A2H and MYD15A2H from 2003-2022. MOD15A2H is shown in the left column, and MYD15A2H is shown in the right column for each vegetation type.

than MOD LAI CV in most vegetation types, except grasslands and broadleaf croplands. Only in broadleaf croplands did both products' annual mean LAI CV show a significant increase, while other vegetation types showed significant decreases or no clear trend, consistent with Figure 7 (a). For TSS, most vegetation types show no significant trend but fluctuating changes, indicating the sustainable usability availability of both products in the time series. The area with significant trends in MYD TSS is slightly smaller than in MOD TSS, suggesting lower systematic uncertainty in MYD products. Both TSS and LAI CV between the two products differed the most in EBF. Figure 9 shows that the overall consistency of intra-annual variation between the two products is good. The LAI CV decreases and then increases seasonally in most vegetation types, reaching a low value in June-August. Conversely, this pattern is reversed for grasslands. The intra-annual variation between the two products is larger in EBF, with MYD LAI CV being greater than MOD LAI CV in all months except June-July.

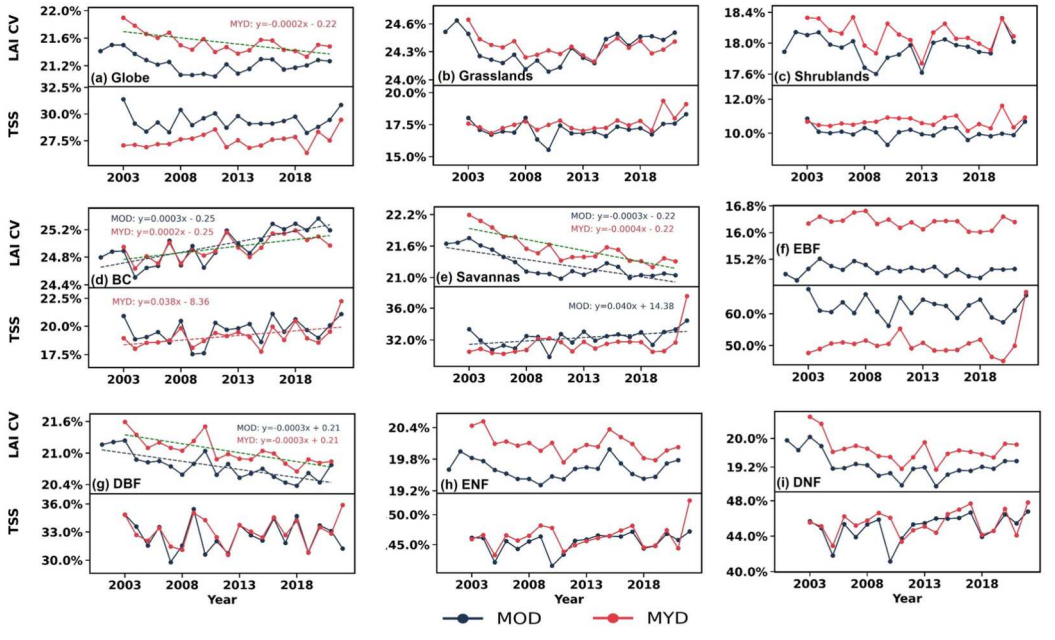

Figure 8. Interannual variations of LAI CV and TSS for different biomes from MOD15A2H (2001-2022), and MYD15A2H (2003-2022). Fitted lines are made for statistically significant trends (Mann-Kendall test, $p \leq 0.05$).

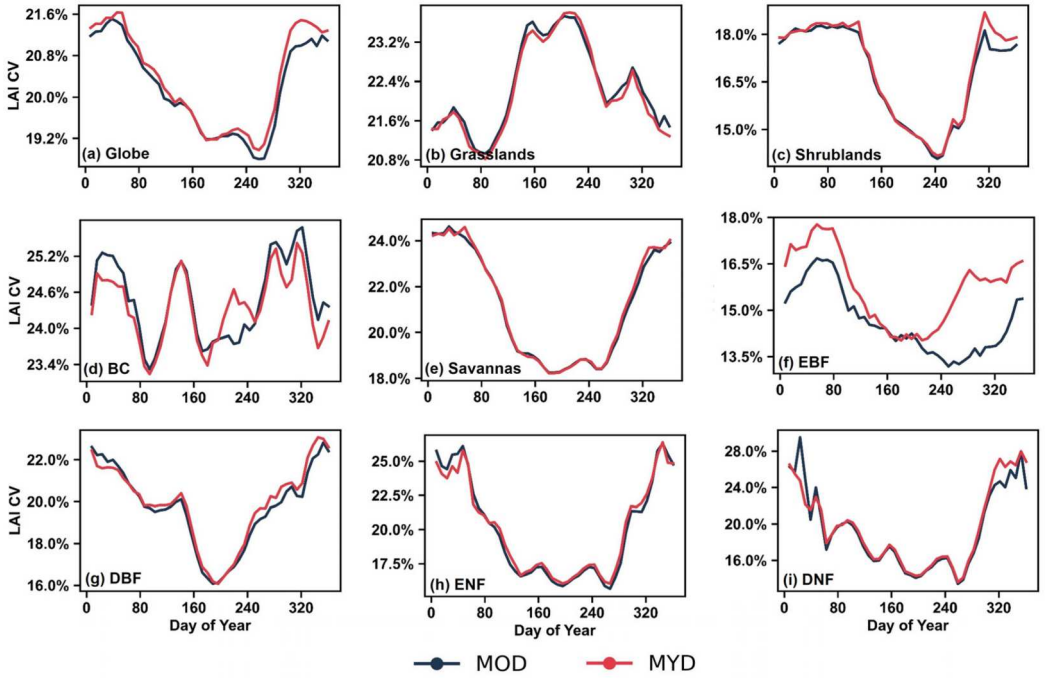

Figure 9. Intra-annual variations of MOD15A2H and MYD15A2H LAI CV for different vegetation types from 2003 to 2022.

4. Discussion

4.1. Drivers for LAI spatiotemporal variability

The spatiotemporal variability of LAI is influenced by various factors, which can be categorized into remotely sensed and non-remotely sensed factors. Remote sensing factors primarily include orbital drift, sensor degradation, the Bidirectional Reflectance Distribution Function (BRDF) effect, atmospheric correction, among others. Apart from the inherent technical differences among satellites and their sensors, they are often impacted by the harsh external environment, resulting in phenomena like orbital drift and sensor degradation, thereby affecting product quality. For example, the orbital drift has led to an increase in the annual average solar zenith angle, particularly causing systematic errors in high albedo regions. Changes in the ground track have reduced the observation frequency within specific time windows, while changes in observation geometry (including sensor zenith and azimuth angles) directly affect the reflectance characteristics of surfaces, leading to significant variations in the BRDF effect and introducing systematic biases (De Beurs and Henebry 2004). Since both Terra and Aqua MODIS have exceeded their 6-year design lifetimes and have experienced significant degradation (Skakun et al. 2018), comprehensive evaluations of the algorithmically improved MODIS products are essential. Due to the continuous movement of the Earth, Sun, and satellites, changes in the relative positions of solar illumination and sensor viewpoints have a noticeable impact on remote sensing observations (Fensholt et al. 2010), known as the BRDF effect. Uncertainty in atmospheric corrections also contributes to the uncertainty in remote sensing observations. Figure 4 illustrates that MOD15A2H LAI and MYD15A2H LAI show the greatest difference in time series stability in broadleaf evergreen forests, which aligns with the findings of previous studies (Yang et al. 2006), due to the limited accuracy of atmospheric corrections. Remote sensing factors contribute to the lack of consistency and stability across products, introducing uncertainties into the analysis of remote sensing time series.

Non-remote sensing factors primarily influence the spatial heterogeneity of LAI, including biotic, abiotic, and anthropogenic factors. Biological factors, such as forest stand density, tree height, and canopy cover, significantly impact the spatial heterogeneity of LAI in forest communities (Bequet et al. 2012; Schleppi, Thimonier, and Walthert 2011; Zhu, Xiang, et al. 2016). Biodiversity is also an important biological factor that influences the spatial heterogeneity of LAI. Variations in vegetation structure, resource utilization, and environmental adaptations among species lead to higher LAI heterogeneity in high biodiversity areas (de Almeida et al. 2021; Oktavia et al. 2022; Peng et al. 2017). In addition to biotic factors, abiotic factors such as topography, climate, and soil characteristics are also important drivers (Prudnikova et al. 2019; Zhang et al. 2015). Anthropogenic factors affect LAI heterogeneity in various ways, including land use, land cover change, and built-up land expansion. Among these, the expansion of built-up land mainly occurs through the occupation of agricultural land (Zhou, Li, and Liu 2020), which corresponds to the highest significant change area in broadleaf croplands shown in Figure 8.

4.2. Causes of product inconsistency

The results of this study provide valuable insights to revisit the consistency of MOD15A2H and MYD15A2H LAI from the perspectives of temporal variability and local spatial heterogeneity. We found that the two products show good consistency in the spatial distribution and overall trend of spatiotemporal variability. However, there are some differences in the degree of correlation and dispersion of spatiotemporal variability, trend magnitude, and area of trend change between the different products. In terms of spatial heterogeneity, the two products showed less correlation in forest biomes compared to nonforest biomes. Compared to MYD, MOD LAI CV is more discrete in long time series, especially in the Amazon, Central Africa, and other broad-leaved evergreen

forests. Time series stability analysis shows MOD TSS is 11.2% higher than MYD TSS in EBF, over three times the difference seen in other vegetation types.

To better understand the spatiotemporal variability differences between MOD and MYD, it is worth exploring their underlying causes further. Three key factors affect the accuracy of LAI retrieval: (1) the uncertainty of the input land cover data, (2) the uncertainty of the models used to construct the lookup tables for the algorithm, and (3) the uncertainty of the input surface reflectance (Yang et al. 2006). For MOD and MYD, which use the same algorithms and land cover data, the third factor is clearly more critical. The MODIS algorithm uses an inversion method based on the Radiative Transfer Equation (RTE). However, inversion calculations can be unstable compared to forward calculations. Small changes in surface reflectance can cause significant variations in LAI values and retrieval instability in the retrieval process. EBF regions have the highest vegetation density, making tropical areas, where EBF is prevalent, a classic challenge in optical remote sensing due to high aerosol conditions and cloud contamination (Shabanov et al. 2005). MOD and MYD observe at different times of day, morning and afternoon respectively, resulting in differences in solar angles and atmospheric conditions. This leads to variations in surface reflectance input data and shadow effects, causing differences in the BRDF effect. This impact is more pronounced in the EBF regions. The MODIS also has limitations in atmospheric correction, and persistent cloud contamination and aerosols in tropical forest regions exacerbate this issue, reducing the accuracy of the input data. The retrieval path of the algorithm is crucial for accuracy. The main algorithm achieves higher precision by matching observed BRFs with simulated BRFs stored in lookup tables and selecting solutions within an acceptable uncertainty range. The average LAI/FPAR values of all solutions are reported as the algorithm output. However, the main algorithm requires high-quality input data for execution. If the uncertainty of the input reflectance data exceeds a preset threshold, a backup algorithm is activated. This backup algorithm is based on the empirical relationship between LAI and NDVI, which cannot guarantee accuracy. In EBF regions, the high vegetation density of forests leads to the NDVI saturation effect, making NDVI ineffective in representing surface vegetation. Poor input data quality typically causes failures in reliable algorithms, but the backup algorithm never fails and its products are almost always generated under poor reference data quality conditions. Fig. S3 shows the correlation density distribution of MOD and MYD LAI CV under different algorithm paths. The R^2 value based on the main algorithm (a) is 0.86, with an RMSE of 0.05 and an RRMSE of 21.85%. The fitted line is almost coincident with the 1:1 line, and the data density is concentrated near the fitted line, indicating a high correlation. In contrast, the R^2 value based on the backup algorithm (b) is 0.55, with significantly higher RMSE and RRMSE compared to those of the main algorithm, at 0.53 and 56.58%, respectively. The data density is also more dispersed, demonstrating noticeably lower consistency and correlation. Therefore, initiating the backup algorithm does not necessarily have similar effects on both products. Specifically, the main algorithm generates results using high-precision input data and a reliable lookup table algorithm, whereas the backup algorithm uses unreliable input data and a limited LAI-NDVI empirical algorithm in inappropriate areas (such as EBF regions prone to NDVI saturation). These results may not accurately reflect the actual surface conditions and are more prone to random errors, leading to differences in the spatiotemporal variability between the two products. Even though Fig. S3c shows that the proportion of the MYD backup algorithm in EBF regions is only slightly lower than that of MOD, it still significantly impacts consistency. Therefore, we primarily attribute the differences in spatiotemporal variability between the two products to the accuracy of the reflectance data.

We also examined the interannual trends and magnitude of change in the spatial and temporal variability of LAI for both products. In terms of spatial heterogeneity, the annual mean MOD LAI CV was smaller in most cases compared to the MYD LAI CV, which had a larger area of significant change. Comparison of TSS trends characterizing temporal stability revealed that over 90% of the vegetated area of both products was free of significant trends, indicating the stability and continuous availability of the products over the time series. These differences are mainly attributed to the difference in transit times between MOD and MYD. Notably, compared to other vegetation types,

broadleaf croplands showed the largest area of significantly trending LAI CV, as well as being the only vegetation type with an increasing trend in annual mean LAI CV. This reflects prior research showing the main driver of the global net leaf area increase since 2000 was cropland greening (33%) (Chen et al. 2019). Analysis of vegetation spatial heterogeneity presents novel insights into the 'Greening Earth' phenomenon and its underlying causes.

4.3. LAI CV trends affected by window size

While using a preset fixed-size window is sufficient for a comprehensive analysis when assessing product consistency, it is also necessary to explore the experimental results using different window sizes. This will allow for a deeper understanding of the spatiotemporal variability of LAI and its trends. Therefore, in this section, MOD15A2H LAI product is used as an example to comparatively analyze the trend of LAI spatial heterogeneity and its proportion under different window sizes (5×5, 11×11, 21×21). Additionally, the results from VIIRS LAI under different window sizes and MODIS LAI based on different resolutions (500 m, 1, 2 km) are also included.

Fig. S4a shows the distribution of trend types for MODIS LAI from 2001 to 2022 under different window sizes. When the window size was increased from 5×5–11×11, the proportion of LAI CV non-significantly trending areas increased in most vegetation types. This was because the expansion of the window range introduced more weakly correlated LAI pixels, resulting in less significant LAI CV trending. However, this proportion decreased in grasslands and broadleaf croplands (BC), where there was a significant increase in the proportion of significantly trending areas. This suggests that the variation in local heterogeneity of LAI from range to size is higher in agricultural fields. Furthermore, when the window size was further increased from 11×11–21×21, the proportion of non-significant trends in most vegetation types increased further. However, the rate of increase slowed down, indicating that the effect of further expansion of the window range on LAI CV was decreasing. Fig. S4b presents the distribution of trend types for VIIRS LAI CV from 2012 to 2022 under different window sizes. Different time intervals were chosen for MODIS and VIIRS due to two main reasons: first, the operational time ranges of the two products are different (2001-2022 and 2012-2022), and analyzing trends based on around 10 years of data has some statistical limitations. Hence, the main operational periods of each product were selected. Secondly, this section focuses on comparing the results under different window sizes. From 5×5–11×11, like MODIS, the proportion of non-significant trends increased in most vegetation types, while it decreased in grasslands and BC. The main difference lies in EBF, where the proportion remained almost unchanged for MODIS but gradually decreased for VIIRS. From 11×11–21×21, the proportion of non-significant trends slightly increased or remained nearly unchanged. Fig. S4c shows the distribution of trend types for MODIS LAI based on different window resolutions (i.e. the resolution of individual pixels in the window). When the resolution increased from 500 m to 1 km, the proportion of significant trends dropped significantly, to half or less of the original proportion. This is primarily because, at finer spatial scales, local heterogeneity is more apparent, and even minor changes can be captured, making the heterogeneity trend more evident. As the resolution increases, the information within a single pixel becomes more mixed, and details of local heterogeneity are smoothed out or lost. When the resolution increased from 1 km to 2 km, the proportion of significant trends remained almost unchanged or changed very little. The main reason is the saturation of spatial scale effects; the details of heterogeneity are fully smoothed out, and the characteristics of heterogeneity trends become stable.

4.4. Limitations and future research

This study included a basic analysis of the differences in spatial heterogeneity of LAI between products with different window sizes. However, future research should include a more comprehensive and in-depth analysis to better understand the effect of window size on inter-product consistency.

Additionally, while we conducted a preliminary analysis of the spatiotemporal variability between products under different algorithmic paths, future studies should comprehensively explore these differences. Future research can also focus on analyzing the effects of internal product consistency and external atmospheric conditions on the spatiotemporal variability of LAI. This can be achieved by selectively using the primary and alternate algorithms or by considering different cloud and aerosol concentrations. Moreover, our current analysis primarily focuses on MODIS products. In subsequent studies, it will be essential to conduct a thorough evaluation of VIIRS, HiQ, SI, and other MODIS-based successor or reanalysis LAI products, as well as LAI products with various spatial resolutions. In terms of indicator selection and research approaches, efforts should be made to further separate the impact of product quality from the real spatiotemporal variability changes on the results.

5. Conclusions

In this study, we revisited the consistency between MOD15A2H and MYD15A2H LAI, focusing on the spatial distribution, degree of dispersion, long-term trend, and interannual variation of LAI spatiotemporal variability. The results showed that MOD15A2H and MYD15A2H had similar spatial distributions of LAI CV in both July and February, with absolute differences within 4% in most areas. Compared to nonforest biomes, the correlation between the two products' LAI CV was lower in the forest biomes, especially in ENF. Regarding temporal stability, the difference between the two products was larger in EBF, where MYD15A2H specifically showed better performance. MOD15A2H exhibited greater anomalous fluctuations in local spatial heterogeneity in areas near the equator, such as the Amazon Forest and Central Africa.

According to the trend analysis of spatiotemporal variability, the long-term trend of LAI CV remained consistent in most cases for both products, with small differences in the areas of different trends. The TSS trend area and interannual time-series trend were not significant in most cases. This suggests that the two products are consistent in capturing trends in spatial heterogeneity of vegetation as well as stable and persistent in time series. Despite the consistency in spatiotemporal variability trends between the two products, it's noteworthy that the MOD15A2H LAI CV significant trend area is generally larger than that of the MYD15A2H (4%), and the MYD15A2H's overall annual mean LAI CV is higher (0.2%). However, due to the systematic nature of this discrepancy and the relatively small difference, the impact on studies related to trend direction is weak. In conclusion, this study emphasizes the assessment of remote sensing products from the perspective of spatiotemporal variability. The results indicate that both products have sustainable usability and overall consistency between them, and that product divergence does not reverse or significantly impact the conclusions of related research. However, it should be noted that there are inconsistencies in a few areas and vegetation types. Based on the higher spatial heterogeneity consistency of the two products using the main algorithm compared to the backup algorithm, as well as the distribution of algorithm retrieval rates, these inconsistencies are mainly due to the lack of precision in reflectance data. Similar phenomena may occur in other products. Therefore, this method can be applied to the assessment of other remote sensing products, and it is recommended that studies use spatiotemporally continuous and high-quality reanalyzed datasets to improve the reliability of the results.

Acknowledgments

The authors would like to thank the editors and anonymous reviewers for the valuable comments, which helped improve this paper.

Disclosure statement

No potential conflict of interest was reported by the author(s).

Funding

This work was supported by the National Natural Science Foundation of China [grant numbers 42192580, 42271356], and the Fundamental Research Funds for the Central Universities.

Data availability statement

The MODIS LAI data can be obtained from https://developers.google.com/earth-engine/datasets/catalog/MODIS_061_MOD15A2H. The MCD12Q1 land cover data can be obtained from https://developers.google.com/earth-engine/datasets/catalog/MODIS_061_MCD12Q1.

ORCID

Kai Yan http://orcid.org/0000-0003-4262-1772
Jinxiu Liu http://orcid.org/0009-0001-3820-8195
Jiabin Pu http://orcid.org/0000-0002-7329-3583
Eduardo Eiji Maeda http://orcid.org/0000-0001-7932-1824
Yuri Knyazikhin http://orcid.org/0000-0002-3116-5719
Ranga B. Myneni http://orcid.org/0000-0002-0234-6393

References

Abdi, Hervé. 2010. "Coefficient of Variation." *Encyclopedia of Research Design* 1 (5): 169–171.

Ahl, Douglas E., Stith T. Gower, Sean N. Burrows, Nikolay V. Shabanov, Ranga B. Myneni, and Yuri Knyazikhin. 2006. "Monitoring Spring Canopy Phenology of a Deciduous Broadleaf Forest Using MODIS." *Remote Sensing of Environment* 104 (1): 88–95. https://doi.org/10.1016/j.rse.2006.05.003.

Bequet, Raphael, Matteo Campioli, Vincent Kint, Bart Muys, Jan Bogaert, and Reinhart Ceulemans. 2012. "Spatial Variability of Leaf Area Index in Homogeneous Forests Relates to Local Variation in Tree Characteristics." *Forest Science* 58 (6): 633–640. https://doi.org/10.5849/forsci.10-123.

Camacho, Fernando, Jesus Cemicharo, Roselyne Lacaze, Frederic Baret, and Marie Weiss. 2013. "GEOV1: Lai, FAPAR Essential Climate Variables and FCOVER Global Time Series Capitalizing Over Existing Products. Part 2: Validation and Intercomparison with Reference Products." *Remote Sensing of Environment* 137:310–329. https://doi.org/10.1016/j.rse.2013.02.030.

Chen, Chi, Taejin Park, Xuhui Wang, Shilong Piao, Baodong Xu, Rajiv K Chaturvedi, Richard Fuchs, Victor Brovkin, Philippe Ciais, and Rasmus Fensholt. 2019. "China and India Lead in Greening of the World Through Land-use Management." *Nature Sustainability* 2 (2): 122–129. https://doi.org/10.1038/s41893-019-0220-7.

Climate Data Records from Environmental Satellites. 2004.

Corpetti, Thomas, Xing Gong, MengZhen Kang, BaoGang Hu, and Laurence Hubert-Moy. 2019. "Time-consistent Estimation of LAI by Assimilation in GreenLab Plant Growth Model." *Computers & Geosciences* 130:57–68. https://doi.org/10.1016/j.cageo.2018.12.004.

de Almeida, Danilo Roberti Alves, Eben North Broadbent, Matheus Pinheiro Ferreira, Paula Meli, Angelica Maria Almeyda Zambrano, Eric Bastos Gorgens, Angelica Faria Resende, et al. 2021. "Monitoring Restored Tropical Forest Diversity and Structure Through UAV-Borne Hyperspectral and Lidar Fusion." *Remote Sensing of Environment* 264:112582. https://doi.org/10.1016/j.rse.2021.112582.

De Beurs, Kirsten M., and Geoffrey M. Henebry. 2004. "Trend Analysis of the Pathfinder AVHRR Land (PAL) NDVI Data for the Deserts of Central Asia." *IEEE Geoscience and Remote Sensing Letters* 1 (4): 282–286. https://doi.org/10.1109/LGRS.2004.834805.

De Kauwe, M. G., M. I. Disney, T. Quaife, P. Lewis, and M. Williams. 2011. "An Assessment of the MODIS Collection 5 Leaf Area Index Product for a Region of Mixed Coniferous Forest." *Remote Sensing of Environment* 115 (2): 767–780. https://doi.org/10.1016/j.rse.2010.11.004.

Doraiswamy, P. C., J. L. Hatfield, T. J. Jackson, B. Akhmedov, J. Prueger, and A. Stern. 2004. "Crop Condition and Yield Simulations Using Landsat and MODIS." *Remote Sensing of Environment* 92 (4): 548–559. https://doi.org/10.1016/j.rse.2004.05.017.

Dufrêne, E., Hendrik Davi, C. François, Guerric Le Maire, Valérie Le Dantec, and A. Granier. 2005. "Modelling Carbon and Water Cycles in a Beech Forest" *Ecological Modelling* 185 (2-4): 407–436. https://doi.org/10.1016/j.ecolmodel.2005.01.004.

Fang, Hongliang, Frederic Baret, Stephen Plummer, and Gabriela Schaepman-Strub. 2019. "An Overview of Global Leaf Area Index (LAI): Methods, Products, Validation, and Applications." *Reviews of Geophysics* 57 (3): 739–799. https://doi.org/10.1029/2018RG000608.

Fang, Hongliang, Chongya Jiang, Wenjuan Li, Shanshan Wei, Frederic Baret, Jing M. Chen, Javier Garcia-Haro, et al. 2013. "Characterization and Intercomparison of Global Moderate Resolution Leaf Area Index (LAI) Products: Analysis of Climatologies and Theoretical Uncertainties." *Journal of Geophysical Research: Biogeosciences* 118 (2): 529–548. https://doi.org/10.1002/jgrg.20051.

Fang, Hongliang, Shanshan Wei, and Shunlin Liang. 2012. "Validation of MODIS and CYCLOPES LAI Products Using Global Field Measurement Data." *Remote Sensing of Environment* 119:43–54. https://doi.org/10.1016/j.rse.2011.12.006

Fang, Hongliang, Yinghui Zhang, Shanshan Wei, Wenjuan Li, Yongchang Ye, Tao Sun, and Weiwei Liu. 2019. "Validation of Global Moderate Resolution Leaf Area Index (LAI) Products Over Croplands in Northeastern China." *Remote Sensing of Environment* 233:111377. https://doi.org/10.1016/j.rse.2019.111377.

Fensholt, Rasmus, Inge Sandholt, Simon R Proud, Simon Stisen, and Mads Olander Rasmussen. 2010. "Assessment of MODIS sun-Sensor Geometry Variations Effect on Observed NDVI Using MSG SEVIRI Geostationary Data." *International Journal of Remote Sensing* 31 (23): 6163–6187. https://doi.org/10.1080/01431160903401387

Gao, Si, Run Zhong, Kai Yan, Xuanlong Ma, Xinkun Chen, Jiabin Pu, Sicong Gao, Jianbo Qi, Gaofei Yin, and Ranga B. Myneni. 2023. "Evaluating the Saturation Effect of Vegetation Indices in Forests Using 3D Radiative Transfer Simulations and Satellite Observations." *Remote Sensing of Environment* 295:113665. https://doi.org/10.1016/j.rse.2023.113665.

Hill, M. J., U. Senarath, A. Lee, M. Zeppel, J. M. Nightingale, R. D. J. Williams, and T. R. McVicar. 2006. "Assessment of the MODIS LAI Product for Australian Ecosystems." *Remote Sensing of Environment* 101 (4): 495–518. https://doi.org/10.1016/j.rse.2006.01.010

Huang, Dong, Yuri Knyazikhin, Robert E. Dickinson, Miina Rautiainen, Pauline Stenberg, Mathias Disney, Philip Lewis, et al. 2007. "Canopy Spectral Invariants for Remote Sensing and Model Applications." *Remote Sensing of Environment* 106 (1): 106–122. https://doi.org/10.1016/j.rse.2006.08.001.

Kala, Jatin, Mark Decker, Jean-François Exbrayat, Andy J Pitman, Claire Carouge, Jason P Evans, Gab Abramowitz, and David Mocko. 2014. "Influence of Leaf Area Index Prescriptions on Simulations of Heat, Moisture, and Carbon Fluxes." *Journal of Hydrometeorology* 15 (1): 489–503. https://doi.org/10.1175/JHM-D-13-063.1

Kerr, Jeremy T., and Laurence Packer. 1997. "Habitat Heterogeneity as a Determinant of Mammal Species Richness in High-Energy Regions." *Nature* 385 (6613): 252–254. https://doi.org/10.1038/385252a0

Knyazikhin, Y. 1999. "MODIS Leaf Area Index (LAI) and Fraction of Photosynthetically Active Radiation Absorbed by Vegetation (FPAR) Product (MOD15) Algorithm Theoretical Basis Document." http://eospso.gsfc.nasa.gov/atbd/modistables.html.

Lafont, S., Y. Zhao, J. C. Calvet, P. Peylin, P. Ciais, F. Maignan, and M. Weiss. 2012. "Modelling LAI, Surface Water and Carbon Fluxes at High-Resolution Over France: Comparison of ISBA-A-gs and ORCHIDEE." *Biogeosciences (Online)* 9 (1): 439–456. https://doi.org/10.5194/bg-9-439-2012

Li, Hanliang, Kai Yan, Si Gao, Xuanlong Ma, Yelu Zeng, Wenjuan Li, Gaofei Yin, Xihan Mu, Guangjian Yan, and Ranga B Myneni. 2023. "A Novel Inversion Approach for the Kernel-Driven BRDF Model for Heterogeneous Pixels." *Journal of Remote Sensing* 3:38. https://doi.org/10.34133/remotesensing.0038

Liang, Shunlin, Qiuxiang Yi, and Jinping Liu. 2015. "Vegetation Dynamics and Responses to Recent Climate Change in Xinjiang Using Leaf Area Index as an Indicator." *Ecological Indicators* 58:64–76. https://doi.org/10.1016/j.ecolind.2015.05.036

Liu, Yibo, Jingfeng Xiao, Weimin Ju, Gaolong Zhu, Xiaocui Wu, Weiliang Fan, Dengqiu Li, and Yanlian Zhou. 2018. "Satellite-Derived LAI Products Exhibit Large Discrepancies and Can Lead to Substantial Uncertainty in Simulated Carbon and Water Fluxes." *Remote Sensing of Environment* 206:174–188. https://doi.org/10.1016/j.rse.2017.12.024.

Lu, Xiaoliang, and Qianlai Zhuang. 2010. "Evaluating Evapotranspiration and Water-use Efficiency of Terrestrial Ecosystems in the Conterminous United States Using MODIS and AmeriFlux Data." *Remote Sensing of Environment* 114 (9): 1924–1939. https://doi.org/10.1016/j.rse.2010.04.001

MacArthur, Robert H, and John W MacArthur. 1961. "On Bird Species Diversity." *Ecology* 42 (3): 594–598. https://doi.org/10.2307/1932254

Myneni, R. B., S. Hoffman, Y. Knyazikhin, J. L. Privette, J. Glassy, Y. Tian, Y. Wang, et al. 2002. "Global Products of Vegetation Leaf Area and Fraction Absorbed PAR from Year one of MODIS Data." *Remote Sensing of Environment* 83 (1-2): 214–231. https://doi.org/10.1016/S0034-4257(02)00074-3.

Myneni, Ranga, Yuri Knyazikhin, and Taejin Park. 2015. "MOD15A2H MODIS/Terra leaf area Index/FPAR 8-Day L4 global 500 m SIN grid V006." *NASA EOSDIS Land Processes DAAC*.

Oktavia, Dina, Arshad Ali, Pil Sun Park, and Guangze Jin. 2022. "Strata-dependent Relationships among Temperate Forest Structure, Diversity, and Growth Rate Along a Local-Scale Environmental Gradient." *Ecological Indicators* 135:108566. https://doi.org/10.1016/j.ecolind.2022.108566.

Padhee, Suman Kumar, and Subashisa Dutta. 2019. "Spatio-temporal Reconstruction of MODIS NDVI by Regional Land Surface Phenology and Harmonic Analysis of Time-Series." *GIScience & Remote Sensing* 56 (8): 1261–1288. https://doi.org/10.1080/15481603.2019.1646977

Peng, Siyi, Bernhard Schmid, Josephine Haase, and Pascal A. Niklaus. 2017. "Leaf Area Increases with Species Richness in Young Experimental Stands of Subtropical Trees." *Journal of Plant Ecology* 10 (1): 128–135. https://doi.org/10.1093/jpe/rtw016.

Privette, JL, RB Myneni, Y Knyazikhin, M Mukelabai, G Roberts, Y Tian, Y Wang, and SG Leblanc. 2002. "Early Spatial and Temporal Validation of MODIS LAI Product in the Southern Africa Kalahari." *Remote Sensing of Environment* 83 (1-2): 232–243. https://doi.org/10.1016/S0034-4257(02)00075-5

Prudnikova, Elena, Igor Savin, Gretelerika Vindeker, Praskovia Grubina, Ekaterina Shishkonakova, and David Sharychev. 2019. "Influence of Soil Background on Spectral Reflectance of Winter Wheat Crop Canopy." *Remote Sensing* 11 (16): 1932. https://doi.org/10.3390/rs11161932.

Schleppi, Patrick, Anne Thimonier, and Lorenz Walthert. 2011. "Estimating Leaf Area Index of Mature Temperate Forests Using Regressions on Site and Vegetation Data." *Forest Ecology and Management* 261 (3): 601–610. https://doi.org/10.1016/j.foreco.2010.11.013.

Shabanov, Nikolay V., Dong Huang, Wenze Yang, Bin Tan, Yuri Knyazikhin, Ranga B Myneni, Douglas E Ahl, Stith T Gower, Alfredo R Huete, and Luiz Eduardo OC Aragão. 2005. "Analysis and Optimization of the MODIS Leaf Area Index Algorithm Retrievals Over Broadleaf Forests." *IEEE Transactions on Geoscience and Remote Sensing* 43 (8): 1855–1865. https://doi.org/10.1109/TGRS.2005.852477

Skakun, Sergii, Christopher O. Justice, Eric Vermote, and Jean-Claude Roger. 2018. "Transitioning from MODIS to VIIRS: An Analysis of Inter-Consistency of NDVI Data Sets for Agricultural Monitoring." *International Journal of Remote Sensing* 39 (4): 971–992. https://doi.org/10.1080/01431161.2017.1395970

Sulla-Menashe, Damien, and Mark A. Friedl. 2018. "User Guide to Collection 6 MODIS Land Cover (MCD12Q1 and MCD12C1) Product." *Usgs: Reston, Va, Usa* 1:18.

Tuanmu, Mao-Ning, and Walter Jetz. 2015. "A Global, Remote Sensing - Based Characterization of Terrestrial Habitat Heterogeneity for Biodiversity and Ecosystem Modelling." *Global Ecology and Biogeography* 24 (11): 1329–1339. https://doi.org/10.1111/geb.12365

Turner, Woody. 2014. "Sensing Biodiversity." *Science* 346 (6207): 301–302. https://doi.org/10.1126/science.1256014

Xiao, Zhiqiang, Shunlin Liang, and Bo Jiang. 2017. "Evaluation of Four Long Time-Series Global Leaf Area Index Products." *Agricultural and Forest Meteorology* 246:218–230. https://doi.org/10.1016/j.agrformet.2017.06.016.

Xu, Baodong, Taejin Park, Kai Yan, Chi Chen, Yelu Zeng, Wanjuan Song, Gaofei Yin, et al. 2018. "Analysis of Global LAI/FPAR Products from VIIRS and MODIS Sensors for Spatio-Temporal Consistency and Uncertainty from 2012-2016." *Forests* 9 (2): 73. https://doi.org/10.3390/f9020073.

Yan, Kai, Taejin Park, Guangjian Yan, Zhao Liu, Bin Yang, Chi Chen, Ramakrishna R. Nemani, Yuri Knyazikhin, and Ranga B. Myneni. 2016. "Evaluation of MODIS LAI/FPAR Product Collection 6. Part 2: Validation and Intercomparison." *Remote Sensing* 8 (6): 460. https://doi.org/10.3390/rs8060460.

Yan, Kai, Dongxiao Zou, Guangjian Yan, Hongliang Fang, Marie Weiss, Miina Rautiainen, Yuri Knyazikhin, and Ranga B Myneni. 2021. "A Bibliometric Visualization Review of the MODIS LAI/FPAR Products from 1995 to 2020." *Journal of Remote Sensing* 2021: 7410921.

Yang, W, NV Shabanov, D Huang, W Wang, RE Dickinson, RR Nemani, Y Knyazikhin, and RB Myneni. 2006a. "Analysis of Leaf Area Index Products from Combination of MODIS Terra and Aqua Data." *Remote Sensing of Environment* 104 (3): 297–312. https://doi.org/10.1016/j.rse.2006.04.016

Yang, Wenze, Bin Tan, Dong Huang, Miina Rautiainen, Nikolay V Shabanov, Yujie Wang, Jeffrey L Privette, Karl Fred Huemmrich, Rasmus Fensholt, and Inge Sandholt. 2006b. "MODIS Leaf Area Index Products: From Validation to Algorithm Improvement." *IEEE Transactions on Geoscience and Remote Sensing* 44 (7): 1885–1898. https://doi.org/10.1109/TGRS.2006.871215

Zhang, Zhengqiu, Yongkang Xue, Glen MacDonald, Peter M. Cox, and G. James Collatz. 2015. "Investigation of North American Vegetation Variability Under Recent Climate: A Study Using the SSiB4/TRIFFID Biophysical/Dynamic Vegetation Model." *Journal of Geophysical Research: Atmospheres* 120 (4): 1300–1321. https://doi.org/10.1002/2014JD021963.

Zhou, Yang, Xunhuan Li, and Yansui Liu. 2020. "Land use Change and Driving Factors in Rural China During the Period 1995-2015." *Land Use Policy* 99:105048. https://doi.org/10.1016/j.landusepol.2020.105048.

Zhu, Zaichun, Shilong Piao, Ranga B. Myneni, Mengtian Huang, Zhenzhong Zeng, Josep G. Canadell, Philippe Ciais, et al. 2016. "Greening of the Earth and its Drivers." *Nature Climate Change* 6 (8): 791–795. https://doi.org/10.1038/nclimate3004.

Zhu, Wenjuan, Wenhua Xiang, Qiong Pan, Yelin Zeng, Shuai Ouyang, Pifeng Lei, Xiangwen Deng, Xi Fang, and Changhui Peng. 2016. "Spatial and Seasonal Variations of Leaf Area Index (LAI) in Subtropicalsecondary Forests Related to Floristic Composition and Stand Characters" *Biogeosciences (Online)* 13 (12): 3819–3831. https://doi.org/10.5194/bg-13-3819-2016

Zou, Dongxiao, Kai Yan, Jiabin Pu, Si Gao, Wenjuan Li, Xihan Mu, Yuri Knyazikhin, and Ranga B Myneni. 2022. "Revisit the Performance of MODIS and VIIRS Leaf Area Index Products from the Perspective of Time-Series Stability." *IEEE Journal of Selected Topics in Applied Earth Observations and Remote Sensing* 15:8958–8973. https://doi.org/10.1109/JSTARS.2022.3214224